

Modelling, Simulation and Characterization of a Supercapacitor in Automotive Applications

V. Castiglia, N. Campagna, A.O. Di Tommaso, R. Miceli, *Member IEEE*, F. Pellitteri, C. Puccio and F. Viola
Department of Engineering
University of Palermo
Palermo, Italy
Email: vincenzo.castiglia@unipa.it

Abstract—The energy storage is one of the most discussed topics among Electrical Vehicles (EVs) research. Currently, supercapacitors (SCs) are collecting even more attention due to their unique features such as high power density, high life cycle and lack of maintenance. In this paper, a brief review of supercapacitor mode suitable for the simulation in automotive applications is identified. The model parameters are estimated and used to simulate the behaviour of a commercial SC bank in different operating conditions. The model is finally validated considering experimental results.

Keywords—supercapacitors, modeling, parameter estimation, energy source.

I. INTRODUCTION

The transition to a sustainable and green transportation is the key to reduce air pollution and CO₂ emissions. In recent years, almost all car manufacturers have begun to introduce at least one electric car model in their product list. One of the biggest obstacles in the spread of Electric Vehicles (EVs), in addition to the so called range anxiety [1], is the high price, largely due to the battery. Moreover, the service life of a battery storage system strongly depends on the operating conditions [2]. In particular, high current peaks, such as those that occur during acceleration and regenerative braking, tend to shorten battery life [3].

Supercapacitors (SCs) can be found in several fields of applications [4-21] and they can represent the solution to increase the energy storage system performances and expected life. SCs main attributes are: higher power density than a battery, fast charge and discharge capability, lack of maintenance, high service life and environmental safety [22]. SCs unique features make them especially suitable for Hybrid Energy Storage System (HESS), both in stationary applications, such as wind power station or distributed power generation systems, and vehicle applications [23], [24]. In order to optimize the design of the energy storage using SCs, a

preventive simulation study is required to verify the performance of the system. Thus, a SC model able to describe with adequate accuracy its terminal voltage is needed [25]. Several modeling approaches have been proposed in the literature, mainly classified in Mathematical Model, Electrochemical Model and Equivalent Circuit Model (ECM). Equivalent circuit models are usually preferred because they can be easily integrated in the power system simulation environment.

This paper is divided as follows: in Section II the three-branch equivalent circuit model, available in literature is presented and described. In Section III, the model parameters are obtained from the manufacturer's datasheet and from experimental tests on the Vinattech, 2.7 V, 100F SC. In Section IV the model is validated using an assembled SC pack and performing the Hybrid Pulse Power Test (HPPT) current profile.

II. SUPERCAPACITORS EQUIVALENT CIRCUIT MODELS

In its simplest form, the SC ECM is composed of a resistor, representing the Equivalent Series Resistance (ESR) of the component, connected in series with a parallel RC branch, representing the capacitance effect of the SC and the self-discharge phenomenon, as proposed in [26]. This kind of model can describe the SC terminal voltage over a time window of few seconds. When it is required to simulate the SC behaviour over larger time windows, a more complex model is needed. Among the models available in literature, the three-branch model seems the most suitable for the simulation of automotive applications.

The three-branch model was presented in [27] and is represented in Fig. 1. The equivalent circuit features three RC series branches, each one with different time constants. The first branch, known also as immediate branch, describes the SC instantaneous behavior. It is composed of a fixed resistor R_1 , a fixed capacitor C_1 and a voltage dependent capacitor C_v . The time constant is in

the range of seconds. The voltage across the first branch fixed capacitor, v_{C_1} can be expressed as

$$v_{C_1} = v_{sc} - i_1 R_1 \quad (1)$$

where:

- v_{sc} is the voltage at the supercapacitor terminal,
- i_1 is the first branch current.

The current in the first branch, considering the voltage dependent capacitor, can be expressed as

$$i_1 = (C_1 + C_v v_{C_1}) \frac{dv_{C_1}}{dt} \quad (2)$$

The second branch, or delayed branch, consists of a fixed resistor R_2 and a fixed capacitor C_2 and has a time constant of a few minutes. The voltage across the second branch fixed capacitor, v_{C_2} , can be expressed as

$$v_{C_2} = v_{sc} - i_2 R_2 \quad (3)$$

where i_2 is the second branch current expressed as:

$$i_2 = C_2 \frac{dv_{C_2}}{dt} \quad (4)$$

The third branch, also called long-term branch is composed of a fixed resistor R_3 and a fixed capacitor C_3 and has time constant of hours. The voltage across the third branch fixed capacitor can be expressed as

$$v_{C_3} = v_{sc} - i_3 R_3 \quad (5)$$

where i_3 is the second branch current expressed as:

$$i_3 = C_3 \frac{dv_{C_3}}{dt} \quad (6)$$

In Fig. 1 equivalent circuit, a fourth branch is added to consider the possibility to add an external balancing resistor R_b .

The total current flowing in the SC terminal can finally be expressed as:

$$i_{sc} = i_1 + i_2 + i_3 + i_b \quad (7)$$

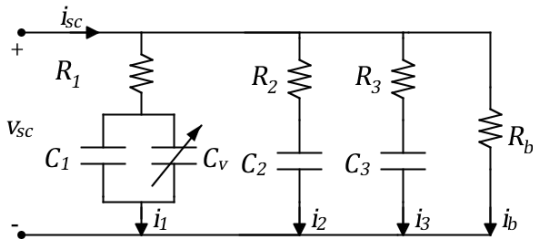


Fig. 1: Three-branch equivalent circuit model.

III. THREE-BRANCH MODEL PARAMETRIZATION

To assess the model performances and accuracy, a test-bench was implemented composed by:

- Vinatech supercapacitors, whose characteristics are reported in TABLE I;
- a Fluke PM2812 Programmable Power Supply, whose characteristics are reported in TABLE II, used to charge the SC;
- an Agilent 6060B Single Input Electronic Load, whose characteristics are reported in TABLE III, used on the discharge phase of the SC;
- a NI 9215 16-Bit Data Acquisition Board (placed in a NI cDAQ 9172 chassis), whose characteristics are reported in TABLE IV, used to acquire the SC voltage and current signal.

All the instrumentation is controlled by a PC connected to the power supply and the electronic load via GPIB and to the NI chassis via USB. The SC voltage signal is acquired at a 10 kS/s sampling frequency and then scaled at a 10 S/s sampling frequency calculating the average value in a 0.1 s time window. All the acquisitions were carried out after the calibration of the board.

At first, the model parameters were estimated using the experimentally acquired data and following the parameter extraction procedure presented in [27]. The parametrization procedure consists on:

- a constant current charge phase of the SC to its rated voltage
- a rest phase, in which the SC is left open circuit for half an hour.

The procedure was applied to different SC to obtain the parameters average values, summarized in TABLE V.

Fig. 2 shows the acquired voltages for different SCs, superimposed to the simulation results using the average model parameters reported in TABLE V. Fig. 3 shows the instantaneous error trend, calculated as

$$Err(t) = v_{sc}(t) - v_{sim}(t), \quad (8)$$

the maximum observed error and the mean error, expressed as

$$Err_{mean} = \sum_{n=1}^N \frac{(v_{sc}(n) - v_{sim}(n))}{N} \quad (9)$$

where N is the number of acquired samples or the simulation steps. It can be noticed that the model fits quite well the four tested SCs voltage response, with a maximum error of 0.11 V and a mean error of 20 mV.

TABLE I: SUPERCAPACITOR DATASHEET SPECIFICATIONS

SPECIFICATION	UNIT	VALUE
Rated Voltage	V	2.7
Rated Capacitance	F	100
AC ESR 1kHz	mΩ	6
DC IR	mΩ	10
Maximum Current	A	65
Leakage Current	mA	0.2
Stored Energy	J	364.5

TABLE II: PM2812 PROGRAMMABLE POWER SUPPLY

	Current	Voltage
Ratings	0 ÷ 10 A	0 ÷ 60 V
Accuracy	± (0.1% + 25) mA	± (0.04% + 20) mV

TABLE III: HP 6060B ELECTRONIC LOAD

	Current	Voltage
Ratings	0 ÷ 60 A	3 ÷ 60 V
Accuracy	± (0.1% + 75) mA	± (0.1% + 75) mA

TABLE IV: NI 9215 ANALOG INPUT MODULE

Signal levels	± 10 V
Sample Rate	100 kS/s
Accuracy	±0.02% ± 1.46 mV
Resolution	16-Bit

TABLE V: SUPERCAPACITOR THREE-BRANCH MODEL PARAMETERS

Parameter	Unit	SC ₁	SC ₂	SC ₃	SC ₄	Average
R ₁	mΩ	7.01	7.03	7.00	6.99	7.00
R ₂	Ω	4.54	2.19	2.07	1.62	1.96
R ₃	Ω	40.96	29.07	28.59	12.73	23.46
C ₁	F	73.26	75.091	76.745	86.00	79.28
C _v	F	23.90	22.57	22.75	11.98	19.09
C ₂	F	45.91	66.12	67.51	58.14	63.92
C ₃	F	58.04	64.47	64.47	61.06	63.33

IV. MODEL VALIDATION OF THE SUPERCAPACITOR BANK

To use the supercapacitors in automotive applications, it is necessary to create banks connecting several in series and parallel to reach the required voltage and current values. The model and the parameters obtained in the previous section are referred to a single SC, but can be extended to the SC bank considering the number of series and parallel connected component N_s and N_p . Specifically, the model simulates the equations for a single supercapacitor, then the bank voltage and current are calculated according to:

$$v_{bank} = N_s \cdot v_{sc} \quad (10)$$

$$i_{bank} = N_p \cdot (i_1 + i_2 + i_3 + i_b) \quad (11)$$

It should be noted that in this way the components are considered identical, whereas they may have slightly different parameters.

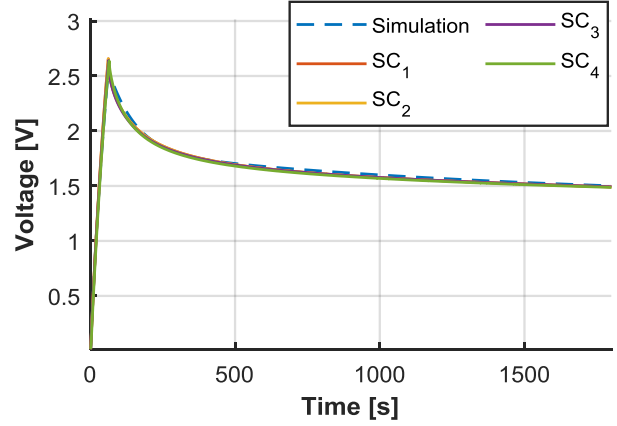


Fig. 2: Simulation vs experimental SC voltage.

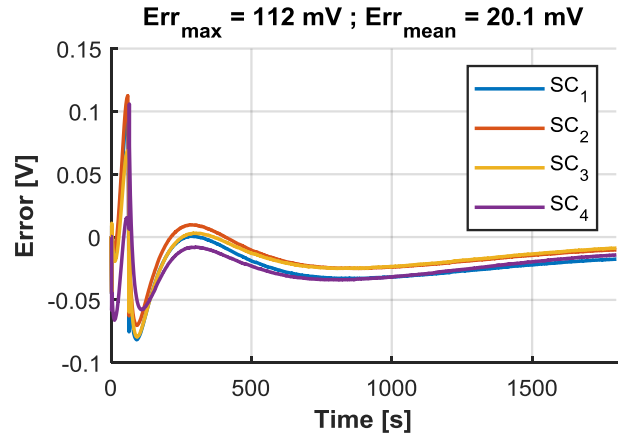


Fig. 3: Instantaneous error trend, and maximum and mean error values.

The assembled SC bank characteristics are reported in TABLE VI. The bank, shown in Fig. 4, is composed of 24 elements in series, each with a 510 Ω resistor in parallel for self-discharge and passive balancing. In the first step for the model validation, the same test performed for the parameter estimation is repeated for the SC bank. In this case, the SC bank was charged to 48 V with 2 A constant current phase. Fig. 5 shows the SC bank voltage response compared to the simulation results and Fig. 6 shows the error trend and report the maximum and mean errors. Despite the simplification to consider all the elements identical, the model estimates with reasonable accuracy the voltage at the SC bank terminals.

A second test, the so-called Hybrid Pulse Power Test (HPPT) was performed on the SC bank. The HPPT consists on alternatively charge and discharge the device under test, with a rest period in between as shown in Fig. 7. Fig. 8 shows both the simulated and experimental voltage and current trends on the SC bank for the HPPT test.

TABLE VI: SUPERCAPACITOR BANK SPECIFICATIONS

SPECIFICATION	UNIT	VALUE
Series components N_s	-	24
Parallel components N_p	-	1
Nominal Capacitance	F	4.17
Balancing resistor R_b	Ω	510
Nominal Voltage	V	60
Nominal Current	A	20

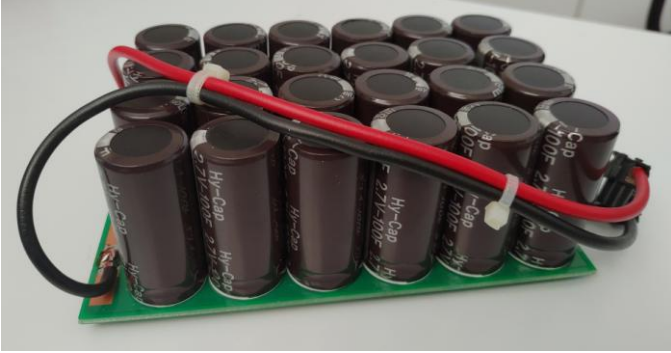


Fig. 4: SC bank used for experimental validation.

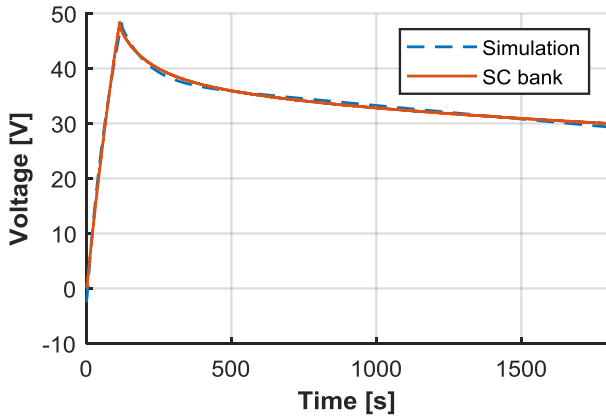


Fig. 5: Simulation vs experimental SC bank voltage.

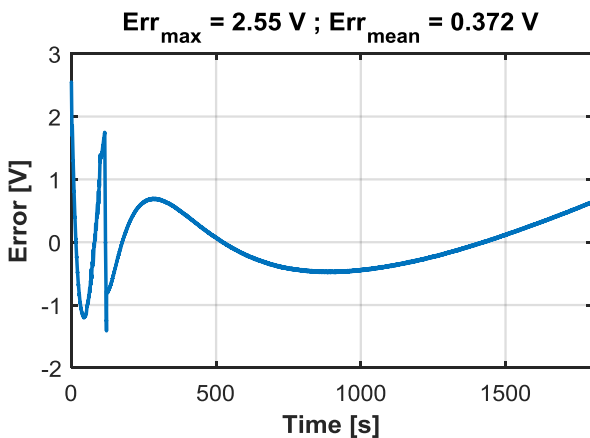


Fig. 6: Instantaneous error trend, and maximum and mean error values for the SC bank.



Fig. 7: HPPT test current profile.

In the first phase, from $t = 0$ s to $t = 120$ s, the SC bank is charged with a constant current up to 48 V. In the second phase, from $t = 120$ to $t = 160$ s, the SC bank is charged with a constant voltage equal to 48 V until the current falls below 0.4 A. In the third phase, the HPPT test begins with the following settings:

- Charge current: 2 A
- Charge pulse duration: 10 s
- Rest period: 10 s
- Discharge current 3 A
- Discharge pulse duration: 10 s

The HPPT test is repeated until the SC bank voltage reaches half of the initial value, i.e. 24 V.

Fig. 9 shows the error trend and report the maximum and mean errors for the SC bank during the HPPT test. The error between the model output voltage and the measurement lies between ± 2 V, and the mean error is equal to 0.91 V, less than 2 % of the maximum observed voltage.

V. CONCLUSION

In this paper a supercapacitor equivalent circuit model for automotive application was identified among those presented in literature. In particular, the three-branch model was used to model the Vinatech, 100 F, 2.7 V Supercapacitor. The model parameters were estimated using several SC and averaged parameters have been used for the simulation of a SC bank composed of 24 series connected elements. Experimental results and simulation results have been compared and discussed. The chosen model has proven to be suitable for the simulation of SC bank in automotive application, predicting the bank terminal voltage with a mean error less than 2% of the maximum observed voltage.

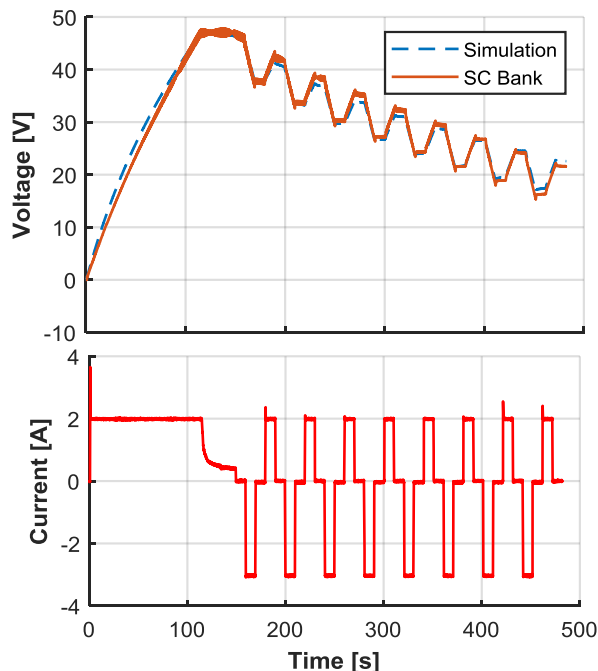


Fig. 8: Simulation vs experimental SC bank voltage and current profile for the HPPT test.

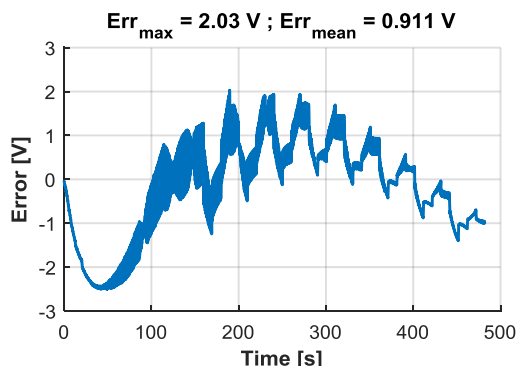


Fig. 9: Instantaneous error trend, and maximum and mean error values for the SC bank during the HPPT test.

VI. ACKNOWLEDGMENT

This work was financially supported by PON R&I 2015-2020 “Propulsione e Sistemi Ibridi per velivoli ad ala fissa e rotante – PROSIB”, CUP no:B66C18000290005, by H2020-ECSEL-2017-1-IA-two-stage “first and european sic eightinches pilot line-REACTION”, by Prin 2017-Settore/Ambito di intervento: PE7 linea C - Advanced power-trains and -systems for full electric aircrafts, by PON R&I 2014-2020 - AIM (Attraction and International Mobility), project AIM1851228-1 and by ARS01_00459-PRJ-0052 ADAS+ “Sviluppo di tecnologie e sistemi avanzati per la sicurezza dell'auto mediante piattaforme ADAS”.

VII. REFERENCES

[1] J. Neubauer and E. Wood, ‘The impact of range anxiety and home, workplace, and public charging infrastructure on simulated

- battery electric vehicle lifetime utility’, *J. Power Sources*, vol. 257, pp. 12–20, Jul. 2014.
- [2] Amal S., R. V. Chacko, Sreedevi M.L, Mineeshma G.R, and Vishnu V., ‘Modelling of ultracapacitor and Power Management strategy for the parallel operation of Ultracapacitor and Battery in Electric Vehicle Configuration’, in *2016 IEEE International Conference on Power Electronics, Drives and Energy Systems (PEDES)*, Dec. 2016, pp. 1–6.
- [3] M. Alhanouti, M. Gießler, T. Blank, and F. Gauterin, ‘New Electro-Thermal Battery Pack Model of an Electric Vehicle’, *Energies*, vol. 9, no. 7, Art. no. 7, Jul. 2016.
- [4] J. Miller, L. B. Sibley, and J. H. Wohlgemuth, ‘Investigation of Synergy Between Electrochemical Capacitors, Flywheels, and Batteries in Hybrid Energy Storage for PV Systems’, 1999.
- [5] Busacca et al, Parametrical study of multilayer structures for CIGS solar cells (2014) 3rd International Conference on Renewable Energy Research and Applications, ICRERA 2014, art. no. 7016528, pp. 964-968.
- [6] Caruso, M., Cecconi, V., Di Tommaso, A.O., Rocha, R. Sensorless variable speed single-phase induction motor drive system (2012) 2012 IEEE International Conference on Industrial Technology, ICIT 2012, Proceedings, art. no. 6210025.
- [7] Caruso, M., Di Tommaso, A.O., Miceli, R., Ognibene, P., Galluzzo, G.R. An IPMSM torque/weight and torque/moment of inertia ratio optimization (2014) 2014 International Symposium on Power Electronics, Electrical Drives, Automation and Motion, SPEEDAM 2014, art. no. 6871997, pp. 31-36.
- [8] Caruso, M., Di Tommaso, A.O., Miceli, R., Galluzzo, G.R., Romano, P., Schettino, G., Viola, F. Design and experimental characterization of a low-cost, real-time, wireless AC monitoring system based on ATmega 328P-PU microcontroller (2015) 2015 AEIT International Annual Conference, AEIT 2015, art. no. 7415267.
- [9] F. Pellitteri, V. Boscaïno, A. O. Di, R. Miceli, G. Capponi, “Experimental test on a Contactless Power Transfer system”, *Ecological Vehicles and Renewable Energies (EVER) 2014 Ninth International Conference on*, pp. 1-6, 2014.
- [10] Pellitteri, F., Caruso, M., Castiglia, V., Miceli, R., Spataro, C., Viola, F., “Experimental Investigation on Magnetic Field Effects of IPT for Electric Bikes”, (2018) *Electric Power Components and Systems*, 46 (2), pp. 125-134.
- [11] L. Schirone, M. Macellari, F. Pellitteri, “Predictive dead time controller for GaN-based boost converters”, *Power Electron.*, vol. 10, no. 4, pp. 421-428, 2017.
- [12] F. Pellitteri, M. Caruso, V. Castiglia, A. O. Di Tommaso, R. Miceli, L. Schirone, “An inductive charger for automotive applications”, *Industrial Electronics Society IECON 2016 - 42nd Annual Conference of the IEEE*, pp. 4482-4486, 2016.
- [13] F. Pellitteri, A. O. Di Tommaso, R. Miceli, “Investigation of inductive coupling solutions for E-bike wireless charging”, *Power Engineering Conference (UPEC) 2015 50th International Universities*, pp. 1-6, 2015.
- [14] Viola, F., Romano, P., Miceli, R., Spataro, C., Schettino, G. Technical and economical evaluation on the use of reconfiguration systems in some EU countries for PV plants (2017) *IEEE Transactions on Industry Applications*, 53 (2), art. no. 7736973.
- [15] Pellitteri, F., Ala, G., Caruso, M., Ganci, S., Miceli, R. Physiological compatibility of wireless chargers for electric bicycles (2015) *International Conference on Renewable Energy Research and Applications, ICRERA 2015*, art. no. 7418629, pp. 1354-1359.
- [16] Caruso, M., Di Tommaso, A.O., Marignetti, F., Miceli, R., Galluzzo, G.R. A general mathematical formulation for winding

layout arrangement of electrical machines (2018) *Energies*, 11 (2), art. no. 446.

[17] Di Tommaso, A.O., Miceli, R., Galluzzo, G.R., Trapanese, M. Efficiency maximization of permanent magnet synchronous generators coupled to wind turbines (2007) *PESC Record - IEEE Annual Power Electronics Specialists Conference*, art. no. 4342175, pp. 1267-1272.

[18] Caruso, M., Di Tommaso, A.O., Imburgia, A., Longo, M., Miceli, R., Romano, P., Salvo, G., Schettino, G., Spataro, C., Viola, F. Economic evaluation of PV system for EV charging stations: Comparison between matching maximum orientation and storage system employment (2017) *2016 IEEE International Conference on Renewable Energy Research and Applications, ICRERA 2016*, art. no. 7884519, pp. 1179-1184.

[19] Schettino, G., Buccella, C., Caruso, M., Cecati, C., Castiglia, V., Miceli, R., Viola, F. Overview and experimental analysis of MC SPWM techniques for single-phase five level cascaded H-bridge FPGA controller-based (2016) *IECON Proceedings (Industrial Electronics Conference)*, art. no. 7793351.

[20] Ala, G., Caruso, M., Miceli, R., Pellitteri, F., Schettino, G., Trapanese, M., Viola, F. Experimental investigation on the performances of a multilevel inverter using a field programmable gate array-based control system (2019) *Energies*, 12 (6), art. no. en12061016.

[21] Di Tommaso, A.O., Livreri, P., Miceli, R., Schettino, G., Viola, F. A novel method for harmonic mitigation for single-phase five-level cascaded H-Bridge inverter (2018) *2018 13th International Conference on Ecological Vehicles and Renewable Energies, EVER 2018*, pp. 1-7.

[22] R. A. Dougal, S. Liu, and R. E. White, 'Power and life extension of battery-ultracapacitor hybrids', *IEEE Trans. Compon. Packag. Technol.*, vol. 25, no. 1, pp. 120-131, Mar. 2002, doi: 10.1109/6144.991184.

[23] Lijun Gao, R. A. Dougal, and Shengyi Liu, 'Power enhancement of an actively controlled battery/ultracapacitor hybrid', *IEEE Trans. Power Electron.*, vol. 20, no. 1, pp. 236-243, Jan. 2005, doi: 10.1109/TPEL.2004.839784.

[24] M. B. Camara, H. Gualous, F. Gustin, A. Berthon, and B. Dakyo, 'DC/DC Converter Design for Supercapacitor and Battery Power Management in Hybrid Vehicle Applications—Polynomial Control Strategy', *IEEE Trans. Ind. Electron.*, vol. 57, no. 2, pp. 587-597, Feb. 2010, doi: 10.1109/TIE.2009.2025283.

[25] K. Saichand and V. John, 'Simplified modeling of ultracapacitors for bidirectional DC-DC converter applications', in *2017 IEEE Applied Power Electronics Conference and Exposition (APEC)*, Mar. 2017, pp. 3134-3141.

[26] L. Zubieta and R. Bonert, 'Characterization of double-layer capacitors for power electronics applications', *IEEE Trans. Ind. Appl.*, vol. 36, no. 1, pp. 199-205, Jan. 2000.

[27] A. S. Weddell, G. V. Merrett, T. J. Kazmierski, and B. M. Al-Hashimi, 'Accurate Supercapacitor Modeling for Energy Harvesting Wireless Sensor Nodes', *IEEE Trans. Circuits Syst. II Express Briefs*, vol. 58, no. 12, pp. 911-915, Dec. 2011.